A Preliminary Investigation of the UHF Properties of LV Cable for WiFi over Power Line Communications

Sean Jordaan[1], Petrus A. Janse van Rensburg[2], Arnold S. de Beer[3], Hendrik C. Ferreira[4], A. J. Han Vinck[5]

University of Johannesburg, South Africa[1,3,4], Walter Sisulu University, South Africa[2], University of Duisburg-Essen, Germany[5].

***Abstract*—In pursuit of a wireless (contactless) power line communications (W-PLC) system for low voltage (LV) power distribution networks, a commonly utilized bundled low voltage electrical cable called Cabtyre, was energized with a range of frequencies up to 3 GHz. The intention was to characterize the cable from a radio frequency radiation perspective for the utilization of standard low voltage distribution cables as antennas in ultra high frequency (UHF) PLC systems. The range of test frequencies extends 550 MHz beyond the present IEEE 802.11g protocol which has a centre frequency of 2.45 GHz and a 80 MHz total bandwidth. The applied tests therefore allow adequately for the maximum bandwidth required with 40 MHz modulation on either side of the 2.45 GHz centre frequency, [1].**

***Index Terms* — Power line communications, wireless, contactless, Bluetooth, IEEE 802.11 wireless protocol.**

I. CONTACTLESS UHF PLC OVER LV CABLE (W-PLC)

Contactless PLC, also called wireless PLC or W-PLC is a new concept, where the (typically) unwanted radiation from PLC systems is actually used as wanted radiation for wireless transmission e.g. WiFi and other UHF systems [3], [4]. Thus the central theme of this paper is the antenna characteristic of a typical LV cable at UHF frequencies. This interest arose out of speculation that the commonly used 30 MHz (or slightly higher) PLC signal [3] is predominantly operating in the transmission line mode for traditional wired signal transfer, which creates and is susceptible to, radio frequency (RF) interference [4]. In this paper, the concept of simultaneously utilizing the electromagnetic interference so generated, for wireless PLC, will be limited to the region outside the near-field radiation sphere as is the norm in controlled radio frequency (RF) communications.

The LV cable tested, was a 2.5 mm^2, three-core, stranded and insulated, spiral-bundled, copper-conductor cable. This cable is commonly called "Cabtyre" and is typically used as a portable low voltage (LV) electrical extension cable at 220 V_{AC}, 15 A. The cable under test was attached to a male bayonet navy connector (BNC) by soldering the earth conductor to the BNC sleeve and any other (one) conductor to the centre terminal of the BNC. The cable under test was then connected to the signal generator BNC output port for measurements. This connection is thus unbalanced, a good condition for radiation, [2].

The connection is also not impedance matched to the cable and neither is the cable (Cabtyre) loaded with its characteristic impedance (Z_o), so, assuming the worst case scenario, the results will therefore only indicate a trend rather than accurately define the observed phenomena. The best result, that is maximum transfer of signal, will occur when the signal generator output port impedance (Z_{out}) equals the load impedance (Z_L), presented by the transmission line, [2], meaning there are no signal reflections from the transmission line back to the input. It will appear as if the line is impedance matched to the source, [2], if no reflections occur when a transmission line, is so lossy or so long that it does not reflect any part of the incident wave.

Equation (1) allows the calculation of the wavelength of the applied 30 MHz signal, as affected by the PVC dielectric surrounding the conductor.

$$\lambda_g = \frac{\lambda_{0(30\text{MHz})}}{\sqrt{\varepsilon_{re}}} = \frac{10000}{\sqrt{6.0917}} = 4051.639 \text{ mm} \quad (1)$$

where λ_g = the wavelength due to the surrounding PVC dielectric and ε_{re} = effective relative permittivity of the PVC insulation surrounding the conductor.

The maximum near-field sphere equation in [5] is therefore adapted to yield (2), which includes both the reactive and the radiation near fields for an electrically large antenna (Antenna length $\geq \lambda/2$), i.e. this sphere will mark the boundary between the near field vs. the far field radiation zone.

$$r_{Nearfield,Max} \leq \frac{2D^2}{\lambda_g} = \frac{2(2024.797)^2}{4051} = 2.024 \text{ m} \quad (2)$$

where λ_g = the wavelength due to the surrounding PVC dielectric, D = the longest dimension of the antenna and, $r_{Nearfield,Max}$ = maximum radius of the near field sphere.

The extent of the near field as calculated by (2) is almost in perfect accord with the observations made in the study by De Beer, [3], in that effective PLC transmission was achieved at a radius of 2 m from the source, at 30 MHz.

According to (2), the near-field boundary of a 2.5 GHz signal must be 25.812 mm from the source of radiation, a figure that renders near field considerations for PLC systems impractical.

The near-field radiation mode (and environment) is not normally considered suitable for radio frequency communication, due to the varying phase relationship between the electric (E) and magnetic (H) fields, [5].

Speculation around the utilization of higher frequency radiation from an LV cable, which can manifest the far-field radiation sphere preferred for radio frequency communication within a few centimeters from the radiating element (LV cable), therefore arose and was consequently physically tested.

Some earlier investigations, [6] considered frequencies between 6 MHz and 11 MHz, a range of frequencies not in common PLC system use.

II. Experiment Layout and Test Parameters

The method of measuring the signal on the Cabtyre, is (1) by means of a direct connection to the end of the cable under test and (2) by contactless measurement via a high frequency dipole antenna (an ETS Lindgren 3180B), placed 1.25m above the cable under test, at various distances from the signal generator output. The Cabtyre cable was 27 m long and was laid out in a straight line on a flat floor surface.

Next, the cable was energized with a swept range of frequencies up to a maximum of 3 GHz, which is in the UHF frequency band and includes the Bluetooth or IEEE 802.11g protocol, centre frequency of 2.45 GHz and its modulation bandwidth.

The instruments used in the physical test were, a Rohde & Schwartz SMC100A signal generator, an ETS Lindgren 3180B dipole antenna and a Rohde & Schwartz FSH3 spectrum analyzer. Fig. 1 shows how these devices were interconnected.

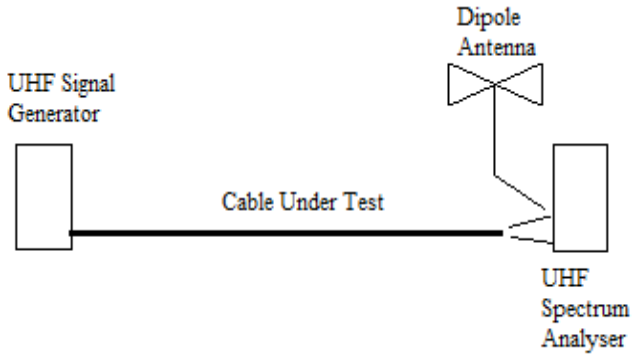

Fig. 1. Graphical representation of the experiment layout.

The conducted signals were measured so that the test antenna terminal voltage ratio versus frequency response (dBμV vs GHz) characterization of the cable could be ascertained.

The level of the radiated (contactless or wireless) radio frequency signal was measured at different points along the Cabtyre cable using a spectrum analyzer via a UHF dipole test antenna. The dipole response results, presented in Fig. 2, are only considered for their flat response perspective and not from a gain perspective.

III. Results Obtained from the Cabtyre Cable UHF Characterizations.

Cabtyre is a spirally bundled, robust, three core, insulated braided copper cable in common use for portable, flexible low voltage electrical distribution such as in an extension cable to operate handheld power machinery remotely from the LV outlet.

A cross sectional diagram of the conductor arrangement is presented in Fig. 3 where each of the three 2.5 mm^2 copper conductors is numbered as 1, 2 and 3.

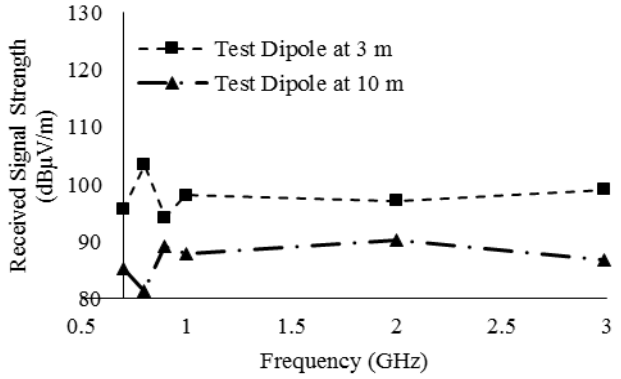

Fig. 2. The ETS Lindgren 3180B test antenna frequency response. Notice the flat response between 1 and 3 MHz.

The spiral bundling of the three conductors implies that they change position with respect to the cable sheath, but not with respect to each other.

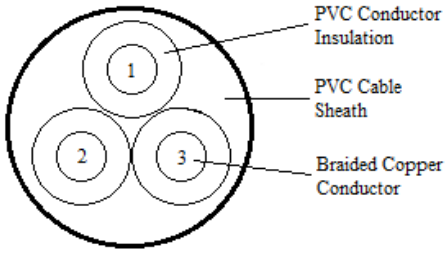

Fig. 3. Cross-sectional view of 3-core Cabtyre spirally bundled LV cable.

As mentioned above, the UHF response of the Cabtyre cable was determined by applying a frequency range from 1 MHz to 3 GHz between the earth conductor and any other conductor.

The Cabtyre cable output voltage versus frequency response in Fig. 4 shows a decline in the level of the measured voltage from that applied to the input of the system, as the frequency increases. This graph is typical of the output voltage versus frequency response characterization of a transmission line as discussed in [8], which models various transmission line (earth and neutral conductor) lengths and paths for frequencies up to 1.4 GHz.

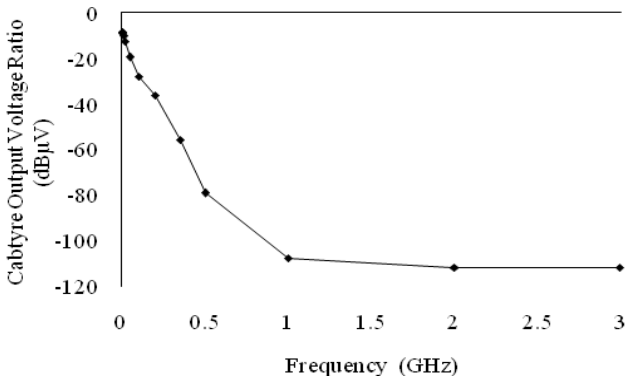

Fig. 4. Amplitude vs. frequency response of 2.5 mm^2 Cabtyre cable, measured at the end of its 27 m length. Notice the typical decay and subsequent linear behavior above 1 GHz.

The decline in the voltage level at the output of the Cabtyre cable, is normally attributed to transmission line real and parasitic resistive and radiation losses, which will prevent any portion of the applied signal reaching the output [2].

The low frequency equation for input impedance (Z_{in}) of a two wire transmission line at a particular frequency is given by (3), which ignores parasitic components as they are only apparent at high frequency, [7].

$$Z_{in} = Z_C \left\{ \frac{Z_L + jZ_O \tan\theta}{Z_O + jZ_L \tan\theta} \right\} [\Omega] \quad (3)$$

where Z_{in} = input admittance of the transmission line, Z_o = line characteristic impedance, Z_L = impedance of loaded (output) port, and θ = separation between input and load in degrees.

At microwave frequencies, however, the standard transmission line input admittance equation must additionally consider the parasitic input impedance (resistance and reactance), or admittance (conductance and susceptance) between the conducting plane and the earth plane.

$$Y_{in} = G_1 + jB_1 + Y_C \left\{ \frac{G_1 + j[B_1 + Y_c(\tan\beta(l_a + \Delta l))}{[Y_c + B_2 \tan(\beta(l_a + \Delta l))] + jG_2 \tan(\beta(l_a + \Delta l))} \right\} \quad (4)$$

where Y_{in} = input admittance of the transmission line, G_1 = conductance of the input port, B_1 = susceptance of input port, G_2 = conductance of the input port, B_2 = susceptance of input port, Y_c = characteristic impedance of the transmission line, β = phase constant of applied signal in the PVC insulation, and Δ_l = length of the fringing effect.

The microwave frequency version (4), of the standard transmission line input impedance equation, (3), is more complex and is in parallel form due to the predominant effect of the parallel parasitic components.

The 1 GHz parameter also marks the boundary at which the Cabtyre cable ceases to become an effective transmission line, or conductor of current. It must therefore also mark the boundary of the discarding of low frequency transmission line theory and the adoption of microwave frequency transmission line theory to explain the trend of the measured quantities.

According to (5), the free space wavelength at 2.45 GHz is 122.449 mm.

$$\lambda_0 = \frac{c_0}{f_0} = \frac{3 \times 10^{11}}{2.45 \times 10^9} = 122.449 \text{ mm} \quad (5)$$

where λ_0 = free space wavelength of applied signal, c_0 = propagation speed of electromagnetic wave in free space and f_0 = frequency of applied signal.

This implies that any air-dielectric conductor that is 122.449 mm long, or longer (equating to the wavelength of 2.45 GHz in free space), which has frequencies of 2.45 GHz and above applied to it, can be considered a transmission line and must be electrically treated as such.

Transmission line theory forms part of microwave frequency theory in that the wavelength of the applied frequency becomes electrically very short in comparison to the length of the conductor to which it is applied.

Fig. 5 shows the radiation from the end of the 27 m Cabtyre cable, measured using the dipole test antenna. A separation of 1.25 m, which equates to the radius dimension, d in (7), was maintained between the antenna and the cable end. This is a dimension greater than ten free space wavelengths of the applied signal, which ensures that any measured signal is not within the near field radiation sphere.

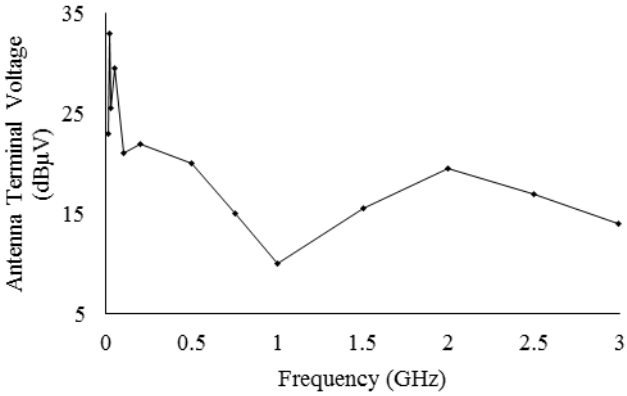

Fig. 5. The energy radiated from the end of the 27 m length of 3-core Cabtyre cable with 1.25 m contactless separation.

IV. Analysis of the Results Obtained from Testing the Cabtyre Cable at UHF

Firstly, the variation of the cable input impedance with frequency, undoubtedly plays a role in the trend of the test antenna terminal RF voltage (E_{Rad}) curve in Fig. 5, which incorporates the effects of the test antenna gain, the test antenna impedance and the spectrum analyzer terminal impedance.

Table I clarifies the relationship between the applied frequency, the input impedance (Z_{in}) and the signal radiated from the end of the cable which results in the test antenna terminal voltage (E_{Rad}) at 50 Ω. It can be seen from Table I that as the absolute value of the input impedance (Z_{in}) approaches 50 Ω, with an absolute magnitude of 24.486 Ω, at 2 GHz, the test antenna terminal voltage peaks. Both the 1 GHz and 3 GHz signals produce lower voltage levels because the absolute value of the input impedance at those frequencies is 271.507 Ω and 144.049 Ω, respectively.

TABLE I
Z_{IN} AND E_{RAD} VS FREQUENCY FOR CABTYRE CABLE

Applied Frequency	Z_{in} for Cabtyre Using (5)	$\lvert Z_{in} \rvert$	Measured RF Voltage Ratio (E_{Rad})
1 GHz	6.896 - j271.494 Ω	271.507 Ω	10 dBµV
2 GHz	0.42 + j24.345 Ω	24.486 Ω	19.5 dBµV
3 GHz	5.7003 – j143.936 Ω	144.049 Ω	14 dBµV

Secondly, the formation of multiple radiation lobes due to multiple wavelengths appearing on what is essentially a long wire antenna (i.e. the LV cable), cannot be disregarded. The concept of radiation lobes is graphically expanded in Fig. 6 which compares the lobes formed as the number of standing

half wavelengths increases on a long wire antenna from 7.75 λ (left hand portion of Fig. 6) to 8 λ (right hand portion of Fig. 6) of the applied signal, [10].

It follows then that a long wire antenna, such as the one created by the application of UHF signals to the 27 m Cabtyre cable, will have many half wavelengths of the 1 GHz (150 mm) to 3 GHz (50 mm) applied signal existing along their length.

The number of free space half wavelengths existing on the LV cable due to the dielectric, is calculated by (6), which reveals that the 1 GHz applied signal produces 426.580 half wavelength cycles, the 2 GHz signal produces 870.777 half wavelength cycles and the 3 GHz signal produces 1190.607 half wavelength cycles.

$$N_{\lambda_g/2} = \frac{2L\sqrt{\varepsilon_{re}}}{\lambda_0} = \frac{2L}{\lambda_g} \tag{6}$$

where $N_{\lambda_g/2}$ = number of half wavelengths of the applied frequency, L = total antenna length, λ_0 = free space wavelength of applied frequency, λ_g = wavelength of applied signal due to the PVC dielectric and ε_{re} = effective relative permittivity of the PVC.

For a standing wave antenna (an antenna which reflects the applied signal due to a load mismatch) symmetrical lobes are produced around the centre of the long wire antenna length (as in Fig. 6) and for a traveling wave antenna (an antenna whose load absorbs all of the applied signal) unsymmetrical lobes are produced in the direction of the current flow, with the largest lobe in that direction and the smallest in the opposite direction, [10].

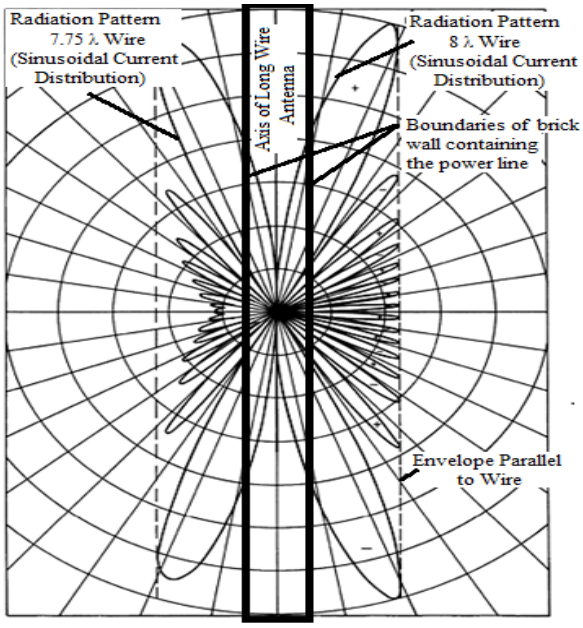

Fig. 6. Radiation lobes as a function of frequency on long wire antennas, [10].

$$E_{E\text{-}Field} = \frac{\sqrt{30 \times P_T \times G_T}}{d} \text{ [V/m]} \tag{7}$$

where, E = radiation E-field strength, P_T = transmission power, G_T = total antenna gain, d = distance the receiver is from the transmitter.

It therefore follows that, since the magnitude of the E-field measured at a fixed distance d from the radiated power source increases after 1 GHz (as displayed by Fig. 7), the transmission line system is most probably beginning to behave as an antenna with the gain G_T, being attributed to radiation lobe directivity, radiation lobe -3 dB beamwidth and radiation lobe density in a multi-lobe environment, [10], [11].

Further, as the applied frequency increases, the greater the number of radiation lobes increases and the smaller the angle between the main radiation lobe and the long wire antenna axis becomes. This implies that a test antenna mounted directly in front (i.e. along the long wire antenna axis) of the LV cable will experience an increase in gain as the applied signal increases and the main radiation lobes focuses on the long wire antenna axis. Greater focus equals greater gain since the beamwidth decreases, [9].

A third consideration must be the frequency response of the reference (test) antenna, as shown in Fig. 2, which increases by 25 dBμV between 2 GHz and 3 GHz at a measuring range of 27 m. Thus the reference antenna gain may have been influenced by the log periodic antenna characteristics, therefore more credibility is placed on the test antenna terminal voltage due to radio frequency radiation from the end of the open circuited Cabtyre cable. This terminal voltage is measured in dBμV which is a logarithmic ratio of voltages referred to 1 μV. In comparison to Fig. 5 which plots the energy radiated against the applied range of frequencies, Fig. 7 plots the value of the E-field against the same frequency range (both at the end of the cable). The peak at about 750 kHz is unexplained, however it is of little interest to the study of the 1 GHz to 3 GHz frequency band centered on 2.45 GHz.

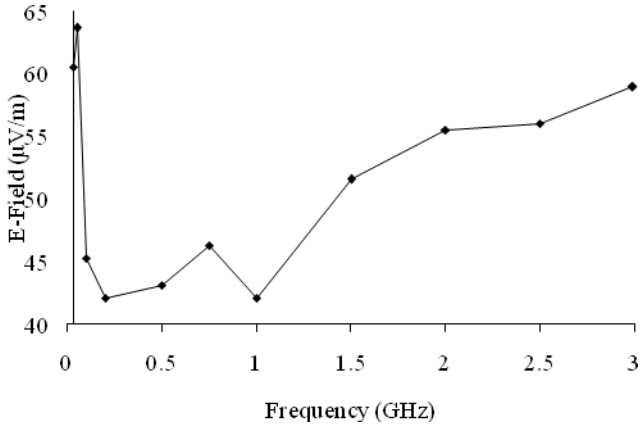

Fig. 7. E-field at the end of a 27 m length of 3-core Cabtyre cable with 1.25 m contactless separation.

In order to create a comparison, radiated energy measurements were next taken at 3 m from the signal generator and also at 10 m from the signal generator, along the

27 m Cabtyre cable / long wire antenna. Only the 3 m results will be discussed, since the trend, as the distance from the signal generator output port increases, is expected and predictable.

Fig. 8 reveals that the received (antenna measured) level at a distance of 3 m from the signal generator output port along the 27 m Cabtyre, is about 20 dBμV higher than that measured at the end of the cable (which is depicted in Fig. 5).

This variance could be attributed to the decay in voltage level with distance. The decay in voltage with distance indicates that the Cabtyre transmission line is in traveling wave mode for the applied UHF signal of 2.45 GHz. This in turn implies that the voltage and current levels decay exponentially, as shown in Fig. 4, and that the radiated signal will weaken as the Cabtyre cable increases in length, until it is too weak for practical application.

A standing wave would have a constant peak level and thus a constant peak level of radiation along the length of the Cabtyre cable, less the radiation and dielectric losses.

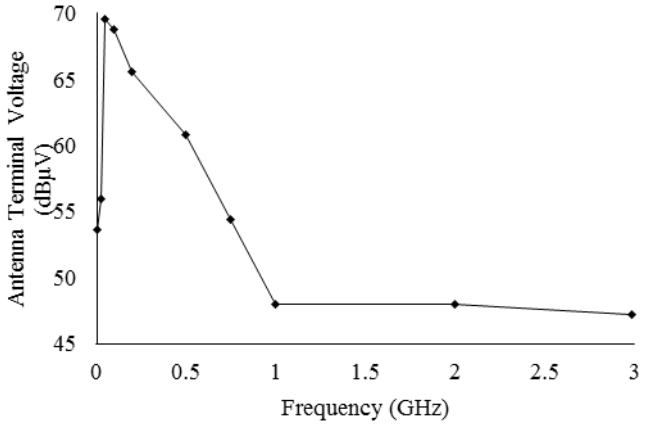

Fig. 8. Radio frequency radiation 3 m from the Cabtyre cable input.

The minimum level of transmitted signal that a radio frequency receiver is able to detect and utilize efficiently is known as the receiver sensitivity. This is technically stated, in [11], as "a good sensitivity to the minimum power at the antenna for a given bit error rate (BER)".

The received electric radiation intensity levels of between 47 dBμV and 48 dBμV measured from 1 GHz to 3 GHz, as displayed by Fig. 8, is considered good since the requirement, in [11], is -76 dBm for the IEEE 802.11b protocol and -92 dBm to -20 dBm for the IEEE 802.11g protocol.

These levels translate, by (8), (9) and (10) to -89 dBμV and also from -105.01 dBμV to -33.01 dBμV respectively for acceptable sensitivity.

$$P_{Rx} = 1\times10^{3}(\text{AntiLog}\frac{\text{Sensitivity}_{dBm}}{10}) \quad [\text{W}] \tag{8}$$

$$V_{Rx} = \sqrt{V_{Rx}\times R_{Term}} \quad [\mu\text{V}] \tag{9}$$

$$\text{Sensitivity} = 20\log\left[\frac{V_{Rx}}{1\times10^{-6}}\right] \quad [\text{dB}\mu\text{V}] \tag{10}$$

where, P_{Rx} = the minimum received power level, V_{Rx} = the minimum voltage at the receiver input for a presumed 50 Ω termination, and sensitivity = minimum functional receiver level.

Since these minimum required levels are much lower than that available from the Cabtyre radiation test the test is considered successful enough to motivate further investigation and study: The radiation level intensity of 47 dBμV equates to approximately 0 dBm by (11) and (12). The initial Cabtyre radiation test level is thus a substantial 105 dBm above the minimum requirement.

$$V = 1\times10^{-6}\left\{\text{Antilog}\frac{\text{dB}\mu\text{V}}{20}\right\} \tag{10}$$

$$A_{dBm} = 10\log\left\{\frac{\frac{V^2}{R}}{1\times10^{-3}}\right\} \tag{11}$$

where V = voltage at any point, A_{dBm} = power gain referred to 1 mW.

A final consideration is the that radiation is facilitated by the fact that adequate radiation is obtained from a quarter wave long radiation element, this means that as the frequency increases and the separation between the energized conductors begins approaching a quarter wavelength of the applied signal, the radiation level will increase.

The E-field magnitude (Fig. 9) is almost double that radiated from the end of the 27 m Cabtyre (Fig. 7), which could again be attributed to the Cabtyre long wire antenna gain, G_T, which is due to radiation lobe orientation with regards to the measuring equipment since there is a greater concentration of radiation lobes per unit square along the side of the cable under test than directly in front of the open circuited transmission line (Cabtyre) termination, [10]. See Fig. 6.

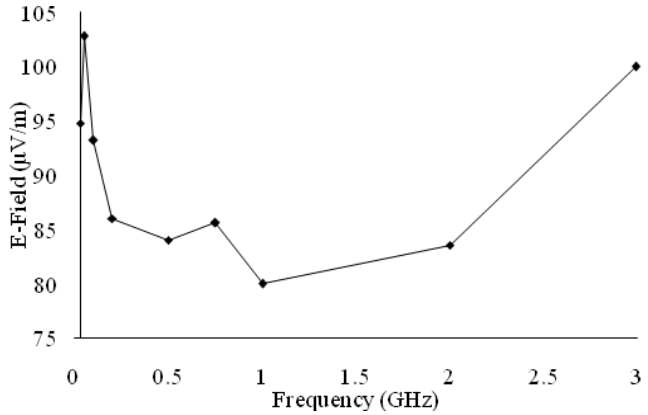

Fig. 9. E-field at 3 m along the 27 m length of Cabtyre cable and 1.25 m contactless separation from cable.

In short, the higher the frequency the more the Cabtyre cable behaves as an antenna and the more it radiates. Transmission line theory predicts that the further the two conductors are apart, the better they will radiate, with the boundary condition for separation, after which radiation is expected, being one half a wavelength, [3]. It follows then, from (12) that, since the separation between the conductors in

Cabtyre cable is 1.6 mm, it would theoretically radiate at 93.75 GHz.

$$f_{Rad} = \frac{c_0}{\lambda_{Applied}} [Hz] \quad (12)$$

The above statements about the frequency at which the Cabtyre cable would radiate effectively, are further dependent on all the typical transmission line losses and design considerations.

The approximately 17 μV/m increase in the E-field that was calculated between 2 GHz and 3 GHz should then also be attributed to radiation lobe concentration since, the more half wavelengths exist on a long wire antenna (as is the case when the applied signal frequency increases to 3 GHz), the more radiation lobes are formed and less nulls occur. In fact, the null ranges are compressed and overlapped by adjacent radiation lobes, meaning more points of measurement / reception are available.

The practical implication of the proliferation of radiation lobes is that continuous reception will be possible in a room, parallel to the Cabtyre cable / LV long wire antenna axis, as opposed to the lobe and null dependant reception at much lower frequencies.

It is surmised that the LV long wire antenna would function as a traveling wave antenna due to its length causing maximum signal decay (in both directions) and therefore no signal will be present at some distant point on the transmission line away from the signal generator and no reflected signal will be presented to the output of the signal generator.

V. Conclusions and Recommendations.

The results obtained in this preliminary test of Cabtyre bundled LV cable are positive in that they indicate that LV cable can radiate high levels of radio frequency energy in the UHF band.

Notwithstanding that it has been demonstrated by physical experimentation, that LV cable can be used as an antenna in the UHF range from 1 GHz to 3 GHz, considerations such as dielectric heating and other limiting causes preventing radiation have not been extensively examined and are recommended for further investigation.

The factors that are highly likely to play important roles in the optimization and proper characterization of this UHF PLC antenna are, impedance matching, lobe density and generation and the separation between energized conductors versus the quarter to half wavelength dimension of the applied signal such that RF radiation is facilitated.

References

[1] M. Gast, "Frequency Hopping Transmission" in *802.11 Wireless Networks: The Definitive Guide, 2nd* ed. Sebastopol: O'Reilly, 2011, ch. *11,* sec. *802.11 FH details*, ch. *12,* pp. *243*, sec. *Maximum theoretical throughput*, pp. *259.*

[2] R. Blake, "Wave Propagation on Lines" in *Electronic Communication Systems, 2nd* ed. Albany: Delmar, 2002, ch. *14*, sec. *Introduction*, pp. *457*, sec. *Electrical Model of a Transmission Line*, pp. *459*, sec. *Step and Pulse Response of Lines*, sec. pp. *460*, sec. *Variation of Impedance Along a Line*, pp. *479*, sec. *Transmission Line Losses*, pp. *482*, sec. *Radiation Resistance*, pp. *565.*

[3] A. de Beer, "Contactless Power Line Communications", in *18th IEEE International Symposium on Power Line Communications and Its Applications*, Glasgow, Scotland, 2014, pp. 111-115.

[4] A. Emleh, A de Beer, et al, "Interference Detection on Powerline Communications Channel When In-Building Wiring System Acts as an Antenna", in *55th International Symposium ELMAR-2013*, Zadar, Croatia, 2013, pp. 141-144.

[5] T. Lecklider. (2005, October). The World of the Near Field. *Evaluation Engineering.* [Online]. Available from: www.evaluationengineering.com/articles/200510/the-world-of-the-near-field.php.

[6] S. Liu, H. Li, et al, "Power-Line Communication Channel Characteristics Under Transient Model", in *IEEE Transactions on Power Delivery*, vol. 29,no. 4, pp1702-1708, August, 2014.

[7] S. Jordaan, M. Ohanga, "A Miniaturised L1 GPS Patch Antenna", in *Journal of Communication and Computer*, vol. 8,no. 7, pp. 586-594, July, 2011.

[8] A. Hakini, G. Ellis, "Equivalent Circuit Models for Propagation Analysis of In-Building Power Line Communications System", in *Aces Journal*, vol. 28, no. 6, pp. 469-478, June, 2013.

[9] D. Dobkin, "Antennas" in *Communications Enginering: RF Engineering for Wireless Networks: Hardware, Antennas and Propagation* Burlington, MA, USA: Newness, 2004, ch. *5* sec. *4, Antenna Radiation Patterns*, pp. *202.*

[10] J. Volakis, "Surface Wave Antennas" in *Antenna Engineering Handbook, 4th ed.* New York: McGraw Hill Education, 2012, ch. *10* sec. *10.5, Long-Wire Antennas.* Available from: http://0-accessengineeringlibrary.com.ujlink.uj.ac.za/browse/antenna-engineering-handbook-fourth-edition.

[11] K. Du, M. Swamy, "RF and microwave subsystems" in *Wireless Communications Systems – From RF Subsystems to 4G Enabling Technologies.* New York: Cambridge University Press, 2010,ch. *11* sec. *11.1.1, Receiver performance requirements*, pp. *373-374.*